FILAMENT LATTICE OF FROG STRIATED MUSCLE

Radial Forces, Lattice Stability, and Filament Compression in the A-Band of Relaxed and Rigor Muscle

BARRY M. MILLMAN AND THOMAS C. IRVING
Biophysics Interdepartmental Group, Department of Physics, University of Guelph, Guelph, Ontario, N1G 2W1, Canada

ABSTRACT Repulsive pressure in the A-band filament lattice of relaxed frog skeletal muscle has been measured as a function of interfilament spacing using an osmotic shrinking technique. Much improved chemical skinning was obtained when the muscles were equilibrated in the presence of EGTA before skinning. The lattice shrank with increasing external osmotic pressure. At any specific pressure, the lattice spacing in relaxed muscle was smaller than that of muscle in rigor, except at low pressures where the reverse was found. The lattice spacing was the same in the two states at a spacing close to that found in vivo. The data were consistent with an electrostatic repulsion over most of the pressure range. For relaxed muscle, the data lay close to electrostatic pressure curves for a thick filament charge diameter of ~26 nm, suggesting that charges stabilizing the lattice are situated about midway along the thick filament projections (HMM-S1). At low pressures, observed spacings were larger than calculated, consistent with the idea that thick filament projections move away from the filament backbone. Under all conditions studied, relaxed and rigor, at short and very long sarcomere lengths, the filament lattice could be modeled by assuming a repulsive electrostatic pressure, a weak attractive pressure, and a radial stiffness of the thick filaments (projections) that differed between relaxed and rigor conditions. Each thick filament projection could be compressed by ~5 or 2.6 nm requiring a force of 1.3 or 80 pN for relaxed and rigor conditions respectively.

INTRODUCTION

In an earlier paper (Millman et al., 1983) the application of osmotic shrinking techniques to the filament lattice of skinned vertebrate muscle in rigor was described and the technique was used to measure the forces between filaments in the A-band lattice. Here, we present results obtained by applying the same technique to skinned frog skeletal muscle in the relaxed state and we have compared the results from relaxed muscle with those obtained from muscle in rigor. The results on relaxed muscle have been briefly reported earlier (Millman and Nickel, 1980; Millman and Irving, 1980, 1982, 1986; Millman, 1981, 1986; Irving and Millman, 1983, 1984).

The use of large polymeric molecules to counteract the lattice swelling of relaxed muscle preparations has been reported for mechanically-skinned frog single fibers (Matsubara et al., 1984; Brenner et al., 1984) and for chemically-skinned whole frog muscle (Magid and Reedy, 1980). Similar studies on invertebrate muscle—mechanically-skinned single-muscle fibers of striated crayfish muscle have been reported (April and Schreder, 1979; April and Maughan, 1986), and a similar technique has been used to measure the diameter of single fibers (but not the lattice spacings) from frog muscle which have been mechanically-skinned under oil (Godt and Maughan, 1977; Maughan and Godt, 1981). In most of the studies where lattice spacing was measured, only a limited range of osmotic pressure was examined; the polymer concentrations used were those which kept the filament lattice near its in vivo spacing. While this is the spacing range of most importance to muscle physiologists, the present study, using a wider range of pressures, has enabled us to gain greater insight into the forces acting on filament lattice of intact muscle. This is necessary if one is to draw conclusions about the state of the lattice and the nature of forces acting on it in vivo (e.g., Elliott and Rome, 1969; April and Wong, 1976; Schoenberg, 1980; Matsuda and Podolsky, 1984; Matsubara et al., 1984). We have been able to model lattice spacings assuming an electrostatic repulsive force together with a weak linear attractive force. Comparison of calculations with experimental data have indicated changes in the lattice structure, particularly in the thick filament structure, under changing external conditions. Using this information, we have been able to model filament lattice dimensions under relaxed and rigor conditions, at short and very long sarcomere lengths.

METHODS

The methods used for applying and measuring external osmotic pressure, for measuring lattice spacings and for calculating electrostatic pressures

were the same as those described in the earlier paper (Millman et al., 1983) and fuller details are given there.

Chemically-skinned muscles were prepared from frog sartorius and semitendinosus muscles. Muscles were dissected from medium-sized (10–12 cm) specimens of *Rana pipiens*. Each preparation was adjusted to the desired sarcomere length and mounted on a perspex frame which could be inserted into a chamber with mylar windows and a fluid capacity of ~15 ml. For relaxed preparations, the freshly dissected muscles were soaked at 4°C for 8 to 10 h in a Ringer's solution containing 5 mM EGTA and no calcium (EGTA equilibration solution: Table I). Muscles were then placed in relaxing solution (Table I) for 15 to 20 m to ensure relaxation of the muscles after membrane depolarization by the high potassium concentration. Triton X-100 was added to a final concentration of 0.5% and the pH adjusted to 6.5 or 6.8. Muscles were skinned at 4°C either in the x-ray chamber with a small magnetic stirrer for 3 to 5 h (pH 6.5), or in a vial containing two to four preparations (mounted on frames) in 80 ml of solution rotating at 2 rpm for 8 to 24 h (pH 6.8). After skinning, the preparation was rinsed in relaxing solution for ~30 min with two changes of solution to remove the detergent.

Osmotic pressure was applied to the filament lattice by using solutions in which dextran (T200 from BDH Chemicals, Toronto, Canada; molecular weight = 200,000 – 270,000; or T2000 [Pharmacia Fine Chemicals, Div. of Pharmacia Inc., Piscataway, NJ]: molecular weight ~2,000,000) had been added to the bathing solution. Dextran concentrations were measured by a sugar refractometer and converted to osmotic pressure using the calibration from Millman et al. (1983). (Calibration curves for T200 and T2,000 dextrans do not differ significantly.) Lattice spacings were determined by small-angle x-ray diffraction using either mirror-monochromator or single mirror (Ni-coated glass) focussing cameras with specimen-to-film distances between 20 and 40 cm. The x-ray source was a microfocus generator with Cu K_α radiation (either Elliott GX6 rotating anode: Cambridge Instrument Ltd., Cambridge, UK; or Model 800 fixed focus; Jarrell-Ash Div. Fisher Scientific Co., Waltham, MA). Exposures ranged from 0.5 to 1 h for muscles without dextran, 2 to 4 h for dextran concentrations up to 15%, and overnight (~16 h) for dextran concentrations above 15%. All muscle preparations were maintained at a temperature of 8 to 10°C during the x-ray exposures. X-ray patterns were recorded on photographic film (medical no screen NS-5T or DEF5; Eastman Kodak Co., Rochester, NY). Spacings were measured on an optical comparator (Scherr-Tumico, St. James, MN).

Sarcomere lengths were determined to an accuracy of better than 0.1 μm during the experiments by light diffraction using a HeNe gas laser.

Theoretical curves for electrostatic pressure were derived from linearized solutions to the Poisson-Boltzmann equation as described by Millman and Nickel (1980). Thick and thin filaments were assumed to be cylinders of radius (a) with uniform surface charge (ν electrons per unit length) in an ionic medium with dielectric constant ($\epsilon = 80$), charges = $Z_i e$ and ion number density = n_i^0. Pressure (P) was calculated from the electric potential (Ψ), averaged over the line joining lattice points midway between the thick filaments, i.e.,

$$P = \frac{8\pi e^2}{\epsilon(kT)^2}\left[\kappa^2\left(\frac{e\Psi}{kT}\right)^2 + \left(\nabla_\parallel \frac{e\Psi}{kT}\right)^2 - \left(\nabla_\perp \frac{e\Psi}{kT}\right)^2\right]$$

$$\frac{e\Psi_a}{kT} = -\frac{2}{1+\sqrt{1+\left(\frac{\lambda_a}{2a\kappa}\right)^2}}\frac{\lambda_a}{a\kappa}\frac{K_0(r\kappa)}{K_1(a\kappa)},$$

where: K_0 and K_1 are modified Bessel functions.

$$\kappa \text{ (Debye constant)} = \left(\frac{4\pi e^2}{\epsilon kT}\sum Z_i^2 n_i^0\right)^{1/2}$$

$$\lambda \text{ (charge parameter)} = \frac{2e^2|\nu|}{\epsilon kT}.$$

Parameters corresponding to the experimental conditions for charge, Debye constant, and sarcomere length were used in each calculation. The filament charges used were those determined for the appropriate conditions from microelectrode measurements (Naylor et al., 1985; Bartels and Elliott, 1985). The Debye constant (κ) was calculated from the ionic strength (I) ($\kappa = 3.26\sqrt{I}$), which in turn was calculated from the concentrations of the ionic species using the procedure of Perrin and Sayce (1967). Note that the calculation of accurate ionic strengths requires a procedure such as this, which uses dissociation constants for all ionic species. Failure to use such a procedure can lead to underestimation of the ionic strength by as much as 30%, particularly with solutions of low ionic strength containing significant amounts of multivalent ions (e.g., ATP-containing solutions). For all calculations, the thin filament charge and charge diameter used were 12 e/nm and 9 nm respectively.

RESULTS

Preparation of Chemically-Skinned Muscles

The method we have described for preparing chemically-skinned frog muscles has provided a technique for consistently producing good preparations from whole muscles. Such preparations are suitable for experiments involving the penetration of large polymeric molecules into the tissue (though not into the filament lattice). An important part of this method is an equilibration in Ringer's solution containing EGTA before skinning (suggested to us by Dr. J. C. Haselgrove). It is this step which distinguishes our present

TABLE I
SOLUTION COMPOSITIONS (IN MILLIMOLARS)

	KCl	NaCl*	$MgCl_2$	$CaCl_2$	$NaHCO_3$	EGTA	ATP	PO_4	Ionic Strength	pH
Ringer's	2.0	115	—	2.0	2.5	—	—	—	0.12	8.0
EGTA equilibrium	2.0	115	—	—	2.5	5.0	—	—	0.13	8.0
40 mM relaxing	40	—	5.0	—	—	5.0	5.0	15	0.11	7.0
75 mM relaxing*	75	—	6.5	—	—	6.0	6.5	15	0.15	7.0
40 mM relaxing (diluted 1:4)	8	—	1.0	—	—	1.0	1.0	3	0.022	7.0
rigor	100	—	4.0	—	—	—	—	6.7	0.12	7.0

*KAc and $MgAc_2$ used in acetate relaxing solution.

method from previous methods used in this laboratory (Millman and Racey, 1977; Millman and Wakabayashi, 1979) and in others (Magid and Reedy, 1980; Padron and Huxley, 1984). Without the EGTA equilibration, we found that a high proportion (25%–50%) of the preparations either did not shrink in the polymeric solutions or else shifted into rigor. This finding is consistent with the observation (Duncan, 1987) of considerable ultrastructural damage in muscle fibers where free calcium levels were higher than in vivo values. Relaxed, chemically-skinned preparations of whole sartorius muscle can be obtained without an EGTA equilibration, but these need to be carefully screened to eliminate muscles that have slipped into rigor (see below).

Relaxed Muscle at Short Sarcomere Lengths

The equatorial x-ray diffraction pattern of chemically-skinned frog skeletal muscle in relaxing solution at sarcomere lengths between 1.9 and 2.5 μm shows strong, sharp 1,0 and 1,1 reflections which indicate a regular hexagonal A-band lattice with order extending over a large number of unit cells. As dextran concentration in the relaxing solution is increased from zero to more than 20% (corresponding to an external pressure range of 0 to ~1,000 torr), the lattice shrinks (Figs. 1 and 2). Also, the sharpness of the x-ray reflections decreases, especially above 10% dextran, showing that long-range lattice order is decreased at higher dextran concentrations (Fig. 1). For frog sartorius muscle in 40 mM KCl relaxing solution (Fig. 2, *filled circles*), three distinct regions of the pressure/spacing curve can be identified. (*a*) Below 10 torr the spacing is nearly constant at ~47.5 nm. (*b*) Between 10 and 20 torr the lattice spacing decreases rapidly with increasing pressure from 47 to 42 nm. (*c*) At pressures between 20 and 2,000 torr, the lattice spacing decreases linearly with the logarithm of pressure from 42 to 34 nm.

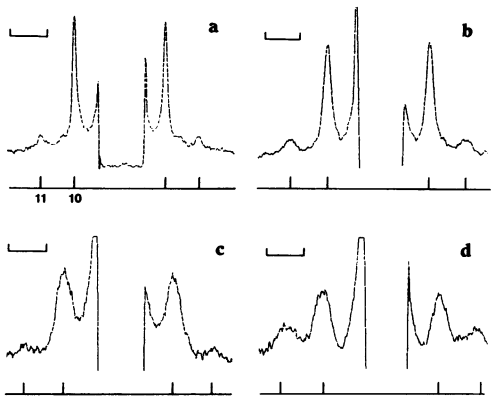

FIGURE 1 Digitized densitometer traces (made with a modified Mark III microdensitometer: Joyce-Loebl and Co., Ltd., Team Valley, Gateshead, England) of equatorial x-ray diffraction patterns taken using a line-focus, single-mirror camera with a specimen-to-film distance of ~28 cm at different concentrations of dextran: (*a*) 0%, (*b*) 3.4% (~18 torr), (*c*) 6.0% (~50 torr), and (*d*) 10.0% (~150 torr). The horizontal calibration lines in the upper left hand corners of each trace correspond to 0.01 nm^{-1}. Both 1,0 and 1,1 reflections can be seen on each trace as indicated by vertical lines.

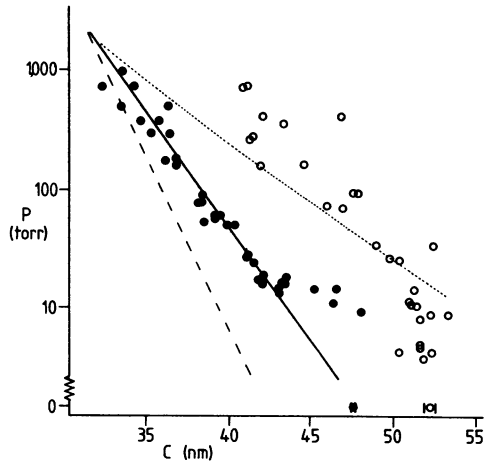

FIGURE 2 A-band lattice spacing (*C*) as a function of externally-applied osmotic pressure (*P*) in frog sartorius muscle at sarcomere lengths between 1.9 and 2.5 μm: in 40 mM KCl relaxing solution (*filled circles*) and in 40 mM KCl relaxing solution diluted 1:4 with distilled water (*open circles*). Each point is an individual experimental measurement except for the data at zero pressure, which are the means with standard error bars from 74 and 23 muscles respectively (from Table II). The lines are electrostatic pressure curves, calculated for thick and thin filament charge diameters of 26 and 9 nm respectively, thick and thin filament charges of 10 and 12 electrons/nm respectively, sarcomere length of 2.2 μm, and Debye constants of 1.07 nm^{-1} (*dashed line*), 0.70 nm^{-1} (*solid line*), and 0.32 nm^{-1} (*dotted line*).

Above 20 torr, the pressure/spacing data lie near, but not over, the curve for electrostatic pressure as a function of interfilament spacing calculated for a thick filament charge of 10 e/nm and charge diameter of 26 nm (Fig. 2, *dashed line*). The thick filament charge we used is one-third of the net charge estimated for vertebrate thick filaments in a relaxing solution corresponding to our conditions of pH and ionic strength (Bartels and Elliott, 1985). It has been estimated (Bartels et al., 1984; Cooke et al., 1987) that one-third of the net thick filament charge lies on HMM-S1, and we have assumed that this reduced charge is that which would produce interfilament electrostatic repulsion.

The slope from the experimental data is less steep than that of the calculated curve; least squares fitting of the data above 20 torr gave an exponential decay constant of -2.0 ± 0.14 nm^{-1}, whereas the theoretical electrostatic pressure/spacing curve for the appropriate conditions had a decay constant of -1.3 nm^{-1}. The data are fit much better by an electrostatic pressure curve calculated using a Debye constant which is reduced by one-third (Fig. 2, *solid line*).

Previous studies of forces between cylindrical rods in

ionic solutions over a range of external pressures (tobacco mosaic virus-Millman et al., 1984; actin filaments—Millman and Bell, 1983), showed good agreement between the experimental data and the calculated electrostatic pressure/spacing curve, though as in the case of the muscle lattice, the slope was generally steeper in the calculated curves (Millman, 1986). Thus, the behavior of the muscle filament lattice when compressed is similar to that of similar gel systems in which the major repulsive forces are electrostatic. The muscle A-band lattice is, however, more complicated than the simple hexagonal gels formed by either tobacco mosaic virus or actin filaments. Not only is the A-band lattice a double array of thick and thin filaments, but the thick filaments are not smooth cylinders. They have projections: heavy meromyosin (HMM), which will tend to interdigitate and reduce the electrostatic force as the filaments are pushed together. Despite the difference between the observed and calculated slopes, repulsive forces in the lattice are consistent with electrostatic forces.

The position of the electrostatic pressure curves depend on both the amount of charge on the rods and the radial position at which this charge is found. Since, in ionic solutions electrostatic forces fall off rapidly with distance, the charge and charge diameter are effectively those of the outermost charges on the filaments. At the high surface charges found in muscle under physiological conditions, the lattice spacing is more dependent on the position than on the amount of the charge (see Millman, 1986, Fig. 4). Electrostatic pressure curves virtually identical to the solid line in Fig. 2 (thick filament charge of 10 e/nm, charge diameter of 26 nm) were calculated for charge and charge diameters of 30 e/nm and 24.2 nm, or 2 e/nm and 30.5 nm.

The muscles used for Fig. 2 were prepared as described in the Methods section with an equilibration in EGTA solution. The intensities of the equatorial x-ray reflections were compared on a qualitative basis (using the scale of Elliott, et al., 1963—$I_{10} \gg I_{11}$, $I_{10} > I_{11}$, $I_{10} \sim I_{11}$, $I_{10} < I_{11}$, $I_{10} \ll I_{11}$) and used to monitor the state of the muscle. When a muscle shifts from relaxation to rigor, there is a concomitant change in the intensities of the 1,0 and 1,1 reflections from the hexagonal A-band lattice such that the intensity ratio (I_{11}/I_{10}) rises (Huxley, 1968). With the EGTA equilibration, control equatorial patterns in relaxing solution without dextran, taken immediately before and after the patterns in dextran always gave patterns in which the intensity of the 1,0 reflection (I_{10}) was greater than that of the 1,1 reflection (I_{11}), indicating that the muscles were relaxed throughout the experiment. Occasionally, meridional x-ray diffraction patterns were obtained from the muscles and these confirmed the conclusions drawn from the equatorial patterns. When $I_{10} > I_{11}$, we observed a meridional diffraction pattern characteristic of relaxed muscle. When, under different conditions (e.g., see below), $I_{10} < I_{11}$, we observed a meridional pattern characteristic of rigor.

In earlier experiments in which an EGTA equilibration was not used, much more variable results were obtained; the spacing data at any pressure showed a great deal more scatter than did corresponding data obtained after an EGTA equilibration and the intensities of the first two reflections ranged from $I_{10} > I_{11}$ (relaxed) to $I_{10} < I_{11}$ (rigor). If only those muscles were considered where the control patterns after dextran had $I_{10} > I_{11}$, the pressure/spacing data described much the same curve as the corresponding data in Fig. 2 (cf. *open circles* and *crosses,* Fig. 3). Where the control patterns indicated full or partial rigor ($I_{10} < I_{11}$), the data lay to the right hand side of the fully-relaxed data, with a clustering of the data over the position of the pressure/spacing curve for rigor muscle.

A few experiments were done using semitendinosus muscles at short sarcomere lengths. It proved more difficult to skin these muscles. (Longer skinning times were required and the muscles tended to go into rigor more readily.) The few results that we obtained were indistinguishable from those obtained with sartorius muscles.

Average spacings over small pressure ranges and the associated standard errors are shown in Fig. 3 for three different conditions where the muscles were fully relaxed, i.e., $I_{10} > I_{11}$. For comparison, similar data from sartorius muscle preparations in rigor are also shown (*filled circles*). The data from relaxed muscle lie to the left of the data for muscle in rigor except at very low pressures where the spacings from relaxed muscle are greater than those from muscle in rigor.

Under zero external pressure (no dextran), the lattice spacing of relaxed muscle is 4–5% greater than that of muscle in rigor (Table II). At an external pressure of ~20 torr, the lattice spacing is the same (44.1 nm) for the two

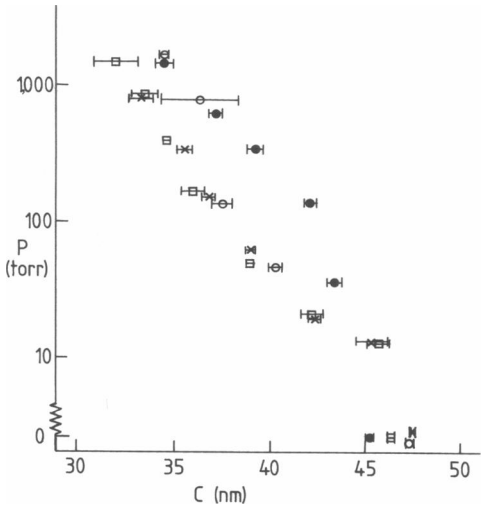

FIGURE 3 A-band lattice spacings (C) averages with standard errors over small ranges of external pressure for frog sartorius muscle at sarcomere lengths between 1.9 and 2.5 μm, relaxed and in rigor. (*Crosses*) 40 mM KCl relaxing solution (data of Fig. 2, *filled circles*). (*Open circles*) 75 mM KCl relaxing solution. (*Squares*) 75 mM K-acetate relaxing solution. (*Filled circles*) rigor solution.

TABLE II
FILAMENT LATTICE SPACINGS AT ZERO EXTERNAL PRESSURE FROM SKINNED FROG SARTORIUS AND SEMITENDINOSUS MUSCLES IN RELAXING AND RIGOR SOLUTIONS

Muscle	Solution	Sarcomere length	Lattice spacing (C)
Sartorius	40 mM KCl relaxing	1.9–2.5	47.6 ± 0.08* (74)‡
Sartorius	75 mM KCl relaxing	1.9–2.5	47.3 ± 0.15 (16)
Sartorius	75 mM KAc relaxing	1.9–2.5	46.4 ± 0.18 (46)
Sartorius	40 mM KCl relaxing (diluted 1:4)	1.9–2.5	52.2 ± 0.37 (23)
Sartorius	rigor (KCl)	2.0–2.5	45.3 ± 0.17 (50)
Semitendinosus	75 mM KCl relaxing	3.6–5.3	40.2 ± 0.8 (14)
Semitendinosus	75 mM KAc relaxing	3.6–4.2	37.1 ± 0.8 (11)
Semitendinosus	rigor (KCl)	3.6–5.4	38.0 ± 0.30 (23)

*Standard error. ‡Number of muscles.

conditions (Fig. 3). This spacing is very close to the lattice spacing found in intact muscle at the corresponding sarcomere length (43.5 nm—Millman et al., 1981). In intact muscle, under physiological conditions, the plasma membrane controls the ionic levels within the cell and thus provides a net pressure on the filament lattice (Matsubara and Elliott, 1972; April, 1975). Furthermore, when the intact muscle moves from the relaxed state to active contraction, the lattice spacing is unchanged (Elliott, et al., 1967; Haselgrove and Huxley, 1973). It thus appears that muscle has evolved so that its lattice dimensions remain unchanged when the intact muscle shifts between relaxed, contracting, and rigor conditions.

Small differences were found in the data from relaxed muscle in different solutions (Fig. 3). The lattice spacings were slightly greater in 75 mM than in 40 mM chloride solution, but the difference was not statistically significant. Lattice spacings were significantly smaller in acetate than in chloride relaxing solution as was originally observed by Magid and Reedy (1980). On average, the lattice spacing in 75 mM chloride relaxing solution containing dextran was 1.7 ± 0.4 nm larger than the mean curve for 75 mM K-acetate relaxing solution. At zero external pressure there was a difference of 0.9 ± 0.2 nm (Table II). The above differences, which are smaller than those reported by Magid and Reedy (1980), could be caused by changes in filament charge, possibly because of chloride binding to the thick filaments as has been suggested by G. F. Elliott on the basis of microelectrode potential measurements (Elliott, 1980).

Muscle at Short Sarcomere Lengths in Low Ionic Strengths Solutions

The lattice spacing of relaxed, skinned muscles increased at all pressures when the preparations were transferred from 40 mM KCl relaxing solution to the same solution diluted 1:4 with distilled water (I = 0.022 M) (Fig. 2, *open circles*). At zero external pressure, the lattice spacing was increased by 4.6 nm (~10%) over the corresponding spacing in full-strength relaxing solution (Table II). A similar increase in lattice spacing with decreasing ionic strength was previously found in rigor preparations, where the changes were found to be consistent with those predicted from electrostatic pressure calculations (Millman et al., 1983). In the case of relaxed muscle at all pressures, the change in lattice spacing is similar, though somewhat greater than that predicted from electrostatic pressure calculations for the change in ionic strength. The electrostatic pressure/spacing curve calculated assuming a Debye constant reduced by one-third (as in the case of normal ionic strength) lies slightly below most of the data (Fig. 2, *dotted line*).

At the lower ionic strength, the 10/11 intensity ratio is lower than at normal ionic strength suggesting that the thick filament projections move towards the thin filaments as the ionic strength is lowered (Brenner et al., 1984; Irving and Millman, 1984; Matsuda and Podolsky, 1984). Skinned rabbit psoas muscles placed in low ionic strength solutions show a similar effect, which Brenner et al. (1984) have interpreted as caused by weakly-bound crossbridges. Our data are consistent with this interpretation. The observation that lattice spacing increased more than predicted from electrostatic calculations in low ionic strength solutions may reflect, in part, this shift towards a rigor-like state. It should be noted, however, that the data in low ionic strength relaxing solution describe a pressure/spacing curve which lies significantly to the right of the data at all pressures from muscle in rigor solution (i.e., no ATP) at normal ionic strength, and the data at low pressure from muscles in low ionic strength rigor solution at the same low ionic strength (0.022M) (Irving, 1983). Thus, the increase in lattice spacing at low ionic strength is, at least in part, a result of the low ionic strength itself, not just a shift from a relaxed to a rigor-like state.

Relaxed Muscle at Long Sarcomere Lengths

Semitendinosus muscle was studied at sarcomere lengths where there was no overlap between the thick and thin filaments (≥3.6 μm). At these long sarcomere lengths, any

electrostatic forces in the A-band arise only from repulsion between thick filaments. Calculations show that where thick and thin filaments do overlap, electrostatic forces between adjacent thick and thin filaments are considerably larger than electrostatic forces between pairs of thick filaments, mainly because thick filaments are closer to thin filaments than to other thick filaments (Millman and Nickel, 1980). Thus, smaller lattice spacings are expected where no filament overlap occurs. As in the case of shorter muscles, the lattice spacing in muscles at long sarcomere lengths decreased with increasing external pressure (Fig. 4). The lattice spacings at long sarcomere lengths lie near the electrostatic pressure curve calculated for a lattice containing only thick filaments with charge diameter of 26 nm. The slope of the calculated electrostatic pressure curve is considerably steeper than that of the experimental data (Fig. 4), the discrepancy being much greater than for shorter sarcomere lengths. At long sarcomere lengths, however, the effect of interdigitating projections from the thick filaments becomes particularly severe, and will cause a substantial reduction in the steepness of the calculated electrostatic pressure curves (Millman and Nickel, unpublished calculations).

At all pressures, the lattice spacing was much smaller in muscles at long sarcomere lengths as compared with muscles at short sarcomere lengths (cf. Figs. 2 and 4). The average from 35 muscles (Fig. 4) of the difference between lattice spacing at long sarcomere length and the corresponding smoothed curve at short sarcomere lengths was 7.2 ± 0.2 nm over the pressure range from 14 to 2,800 torr.

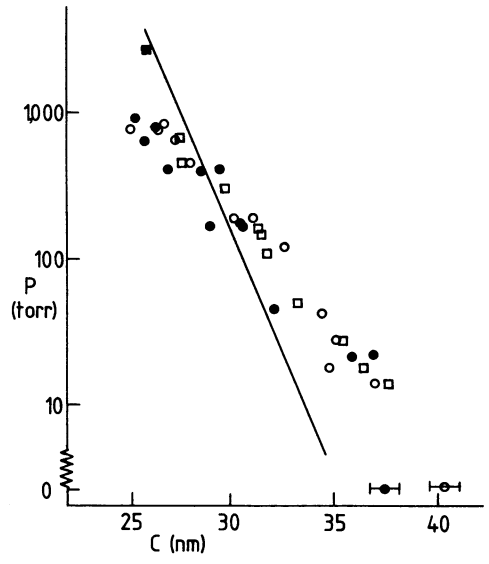

FIGURE 4 Pressure/spacing curve as Fig. 2 for frog semitendinosus muscle at sarcomere lengths ≥3.6 μm. (*Open symbols*) In 75 mM KCl relaxing solution. (*Filled symbols*) In 75 mM KAc relaxing solution. (*Circles*) Data for sarcomere lengths between 3.6 and 4.2 μm. (*Squares*) Data for sarcomere lengths >4.2 μm. The line is the electrostatic pressure curve calculated for a lattice of only thick filaments with charge diameter of 26 nm, charge of 10 electrons/nm and a Debye constant of 0.70 nm^{-1}.

Above 3.6 μm, the lattice spacing did not depend, to any significant extent, on sarcomere length: data at sarcomere lengths >4.2 μm (Fig. 4, *squares*) described the same curve as data at sarcomere lengths between 3.6 and 4.1 μm (Fig. 4, *open circles*). The average difference between lattice spacings at long and short sarcomere lengths (7.2 nm) is the same as the difference between calculated electrostatic pressure curves for 3.6 and 2.2 μm (i.e., an average of 7.2 nm, ranging from 4 to 10 nm) over the same pressure range, using the same values for thick filament charge and charge diameter (10 e/nm and 26 nm respectively).

As was the case at short sarcomere lengths, the filament lattice in 75 mM K-acetate relaxing solution was slightly smaller than in 75 mM KCl relaxing solution, though in this case the difference was not significant statistically. Lattice spacings from twelve muscles in 75 mM K-acetate relaxing solution were on average 0.4 ± 0.25 nm smaller than the mean curve for muscles in 75 mM KCl relaxing solution. A larger (and statistically significant) difference was found at zero external pressure (3.1 ± 1.1 nm: Table II).

We were concerned that with these highly stretched muscles, some sarcomeres contributing to the x-ray diffraction patterns might not be stretched beyond 3.6 μm. Three factors make it unlikely that any significant number of shorter sarcomeres were present: (*a*) all our x-ray diffraction patterns were from the center of the muscle where the sarcomeres tend to be longest (Huxley and Peachey, 1961), (*b*) all of our data showed a dramatic decrease in lattice spacing when compared with data at short sarcomere lengths, a decrease that would be expected theoretically only for muscles stretched beyond 3.6 μm, and (*c*) we observed no difference in spacings for data at sarcomere lengths between 3.6 and 4.1 μm (where short sarcomere lengths would be most likely) as compared with data at sarcomere lengths above 4.1 μm.

Muscle in Rigor at Long Sarcomere Lengths

Semitendinosus muscles, stretched beyond filament overlap, were also examined in solutions without ATP which would have produced rigor at shorter sarcomere lengths where the thick and thin filaments overlap. Average spacings over small pressure ranges were calculated and compared with spacings from muscles at long sarcomere length in relaxing solution (Fig. 5). In the case of muscle in rigor, as the external pressure was increased, the data showed very little change in lattice spacing for pressures up to 100 torr, followed by a nearly logarithmic decrease in spacing as pressure increased from 100 to 2,000 torr (Fig. 5, *filled circles*). The difference between the relaxed and rigor curves at long sarcomere lengths is similar to that found at shorter sarcomere length (cf. Figs. 3 and 5). At the higher pressures, the spacing in rigor solution was greater than that in relaxing solution whereas at low and zero pressure

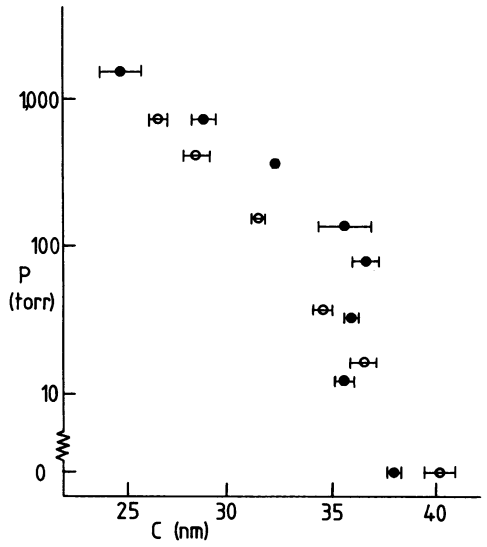

FIGURE 5 A-band lattice spacing (C): averages with standard errors over small ranges of external pressure for frog semitendinosus muscle at sarcomere lengths ≥3.6 μm, in relaxing (*open circles*) and rigor (*filled circles*) solutions.

the spacing was greater in relaxing solution (Fig. 5, Table II). As at short sarcomere lengths, the spacings in relaxing and rigor solutions were the same at an external pressure of ~20 torr (Fig. 5).

At zero external pressure, using muscles skinned for normal periods (3–5 h) in KCl solutions, lattice spacings in relaxing solutions were significantly greater than those in rigor solutions (Table II). However, the spacings observed in relaxing solutions at zero pressure, unlike the spacings at higher pressures, depended on details of the skinning procedure. For example, skinning in relaxing solution for a longer period (~24 h), produced preparations with a smaller lattice spacing—similar to that found for preparations in rigor solution. It is possible, as suggested by Higuchi and Imazume (1986), that lattice swelling at long sarcomere lengths is constrained by an interfibrillar network of noncontractile material and that this is affected differently by different skinning periods, thus limiting the lattice swelling under some conditions. These effects need to be investigated further. Though there were uncertainties at long sarcomere length data at zero external pressure, such uncertainties were not found in the data where external pressure was applied.

MODELING AND DISCUSSION

The Difference in Spacing Between Relaxed and Rigor Muscles

The relationship between lattice spacing and external pressure in relaxed muscle is significantly different from that in rigor muscle; this difference is similar in both short and long preparations (Figs. 3 and 5). The data suggest that the radial stiffness of the lattice differs under the two conditions, being much stiffer in the rigor state. The most logical site for this radial stiffness is the projections from the thick filaments. It is known that during a shift from the relaxed to the rigor state, the projections (HMM-S1 and possibly HMM-S2) move further from the thick filament backbone (Pepe, 1967; Huxley and Brown, 1967). It is likely that these same parts can compress under external pressure.

A more quantitative comparison of the spacing difference between relaxed and rigor muscle is shown in Fig. 6. Here the difference in lattice spacing for the relaxed and rigor lattices ($\Delta C = C[rigor] - C[relaxed]$) is plotted as a function of the (logarithm of the) applied external pressure. The striking feature of Fig. 6 is that the data from both cases describe the same curve: ΔC being negative below 20 torr, positive between 20 and 1,500 torr, and zero at 20 torr (and possibly above 2,000 torr). Because the same curve is found at short sarcomere lengths and at sarcomere lengths beyond filament overlap where no actin-myosin crossbridges can form, the difference between relaxed and rigor curves is unlikely to be caused only by crossbridges linking the thick and thin filaments. It is more likely some property of the thick filament projections which is independent of whether or not the projections are forming crossbridges.

Differences between relaxed and rigor spacings have previously been observed at sarcomere lengths below 3.6 μm, and attributed to the properties of attached crossbridges. Such models have been used to calculate radial forces transmitted by the crossbridges (Maughan and Godt, 1981; Millman and Irving, 1982; Matsubara et al., 1984). A specific model for lattice stability in which both M-lines and crossbridges play a role in stabilizing the filament lattice has been proposed by Matsubara et al. (1984). However, the assignment of spacing differences between relaxed and rigor states to actin-myosin crossbridges and the calculations associated with this assump-

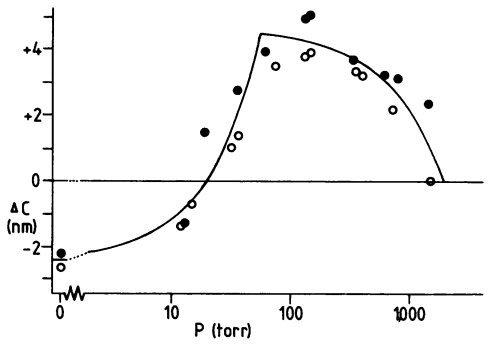

FIGURE 6 Differences in lattice spacing between relaxing and rigor solutions (ΔC = C[rigor] − C[relaxed]) for frog muscle as a function of external pressure. (*Filled circles*) Sartorius muscle at sarcomere lengths between 1.9 and 2.5 μm. (*Open circles*) Semitendinosus muscles at sarcomere lengths ≥3.6 μm. The line is the curve calculated on the assumption that ΔC arises from a difference between relaxing and rigor solutions in the stiffness of the thick filament projections (see text for details).

tion are clearly untenable if the differences are observed whether such crossbridges are formed or not.

A rather different model is outlined below. The model does not assume a specific origin for the forces which resist lattice compression nor about the specific location of these forces, though as discussed later, we favor electrostatic forces. The data from relaxed preparations at low pressure (eg. Fig. 2, *filled circles*) suggest that part of the thick filament structure is readily compressed in the radial direction but is relatively incompressible at higher pressures. It is likely that the parts which compress are the projections which are pushed up against the backbone at pressures above 20 torr. In rigor preparations (Fig. 3), such a highly compressible region is not seen at low pressures, but a compressible region does appear to be present at higher pressures.

We have assumed that in both relaxed and rigor states, the projections (whether attached to thin filaments or not) can be pushed up against the backbone, that higher compressive forces are required in the rigor state, and that in both conditions the force is linearly related to the distance compressed (i.e., the stiffness is Hookean). Two linear curves with four parameters (i.e., radial thick filament compressibility and the pressure where the thick filaments are fully compressed, for relaxed and for rigor preparations) can be used to describe the data of Fig. 6. These parameters were calculated using least squares fitting to a linear plot of the data of Fig. 6 (see eg. Millman, 1986, Fig. 6). The values obtained were $5.4 \pm 0.9 \times 10^{-13}$ m^3/N and 0.42 ± 0.05 N/m^2 for relaxed preparations, and $1.05 \pm 0.20 \times 10^{-14}$ m^3/N and 14.4 ± 1.9 N/m^2 for rigor preparations. The relationship between ΔC and pressure, calculated using the above parameters, is shown as the line in Fig. 6 which clearly provides a reasonable fit to the data. Furthermore, data obtained from glycerol-extracted and chemically-skinned rabbit psoas muscle under relaxed and rigor conditions (Millman, 1981; Millman et al., 1983), is also fit well by the line in Fig. 6 (see Millman, 1986, Fig. 6).

Although the above model accurately predicts the relationship between ΔC and pressure, it also implies that the lattice will swell indefinitely. A small attractive pressure is required to account for the observed lattice equilibrium under conditions of zero external pressure. This attractive pressure may affect the compressibility calculated above for the relaxed condition, but provided the pressure is small, this effect can be removed by constraining the relaxed compressibility so that the relaxed and rigor curves intersect at the observed spacing (i.e., 44.1 nm). If this is done, the relaxed compressibility is increased from 5.4 to 12.5×10^{-13} m^3/N.

If one assumes further that there are six projections (HMM-S1) per 14.3 nm along the thick filament and that the lattice spacing is 43 nm, the radial stiffness per projection is ~0.25 mN/m for relaxed muscle and 30 mN/m for muscle in rigor. Each projection in relaxed muscle can be compressed by as much as 5 nm, requiring a force of 1.3 pN; the corresponding values for rigor muscle are 2.65 nm and 80 pN.

Modeling the Filament Lattice

We have argued elsewhere (Millman and Nickel, 1980; Millman, 1986) that in relaxed muscles, repulsive electrostatic forces are the major internal force system controling lattice spacing whenever a significant external osmotic pressure is applied. Only at very low external pressures do other types of force make significant contributions. This role of electrostatic forces in the relaxed muscle lattice is supported by the observed change in the slope of the pressure/spacing data with ionic strength (Fig. 2) and by the difference in lattice spacing between long and short sarcomeres. In rigor muscle, it has already been shown that the lattice spacings are largely determined by electrostatic forces (Millman et al., 1983). Thus, over most of the pressure range studied, mechanical contributions from the crossbridges are probably small in comparison to electrostatic forces.

If one assumes that the primary repulsive force in both relaxed and rigor states is electrostatic and that the difference in the lattice spacing between the relaxed and rigor conditions arises because of different compressibilities in the two states, it should be possible to set up an appropriate model for the filament lattice and use it to calculate lattice dimensions under a wide range of conditions. We have done this using those parameters that were known from experimental conditions or from the structure of the lattice (i.e., Debye constant = 0.70 nm^{-1}, thick and thin filament effective charges = 10 and 12 e/nm respectively, thin filament charge diameter = 9 nm) and determining the remaining ones by the following steps. (*a*) The data from relaxed muscles at pressures above 20 torr (Fig. 2, curve 1) was compared directly with calculated electrostatic pressure curves to determine the thick filament charge diameter (=26 nm). (*b*) The difference between relaxed and rigor spacings under different external pressures was used as described earlier to calculate the thick filament compressibility and the pressure where minimum thick filament diameter was reached under relaxed and rigor conditions, with the constraint on the relaxed compressibility that the intersection of the relaxed and rigor curves should occur at the spacing observed (44.1 nm). (relaxed = 1.25×10^{-12} m^3/N and 0.42 N/m^2; rigor = 1.05×10^{-14} m^3/N and 14.4 N/m^2). (*c*) Using these parameters, electrostatic pressure/spacing curves were calculated for relaxed and rigor conditions at short (2.2 μm) and at long (3.6 μm) sarcomere lengths. (*d*) Data at zero pressure under both relaxed and rigor conditions were used to calculate an attractive pressure, assuming that the electrostatic pressures calculated at these spacings (in [*c*] above) were balanced by an attractive pressure (the data suggested a linear, increasing pressure = 0 at 20 nm, increasing to 0.24 N/m^2 [32 torr] at C = 48 nm). (*e*) The

net pressure/spacing curve was calculated by subtracting the attractive pressure calculated in (*d*) from the repulsive electrostatic pressure calculated in (*c*) for all spacings where the repulsive pressure was greater than the attractive pressure.

The pressure/spacing curves calculated in this manner were compared with experimental data for both long and short sarcomere lengths and the results are shown in Fig. 7. The calculated curves provide reasonable fits to the data, particularly at shorter sarcomere lengths. The difference between relaxed and rigor conditions is well described and the change in spacing found for both relaxed and rigor conditions in moving from short to long sarcomere lengths is also accurately portrayed. The exact shape of the curves at long sarcomere lengths is less well fit, probably because of interdigitations of the projections as discussed earlier.

If the model for thick filament compression is correct, one should also observe changes in the mass distribution across the lattice as the lattice is compressed; i.e., the mass associated with the thick filament projections should move closer to the filament backbone. We have done detailed Fourier reconstructions of x-ray diffraction patterns obtained for the 40 mM relaxed muscle data (Fig. 2) between 10 and 20 torr (the region where substantial change in filament charge diameter is postulated). Our analysis indicates a strong positive correlation between the full-width-half-maximum of the thick filament electron density and both the lattice spacing (*C*) and the external pressure (*P*), thus providing strong support for compression of the thick filament projections (Irving and Millman, 1985, 1987, and unpublished results).

At low pressures where the lattice spacing does not change appreciably (48 nm for physiological ionic strengths), calculated electrostatic pressures are quite small and we have assumed that these are balanced by an attractive pressure additional to the osmotic pressure. This attractive pressure could result from van der Waals forces, either alone or in conjunction with forces from structural components of the A-band (e.g., the M-lines). The magnitude of the attractive pressure was estimated in step (*d*) above. The analysis suggests an attractive pressure, independent of sarcomere length, which increases with lattice spacing from 20 to 32 torr between 38 and 48 nm. Van der Waals pressures calculated at these spacings by the methods described by Brenner and McQuarrie (1973) using a value for the Hamaker coefficient of 7×10^{-21} J, give pressures of the right order of magnitude, but decreasing with lattice spacing. The pressures calculations depend critically, however, on the exact distribution of thick filament crossbridge mass. On the basis of these experiments, it is not clear whether van der Waals forces alone are sufficient to stabilize the filament lattice or whether additional structural forces must be invoked as well. On balance, it appears likely that some structural contribution is required.

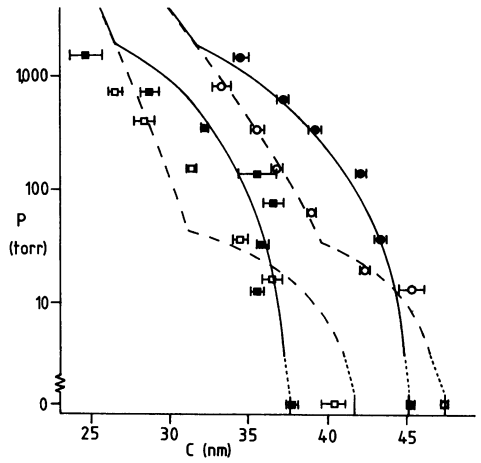

FIGURE 7 Experimental pressure/spacing data compared with calculated model-derived curves. (*Circles*) Frog sartorius preparations at short sarcomere lengths (data from Fig. 3). (*Squares*) Frog semitendinosus preparations at sarcomere lengths ≥3.6 μm (data from Fig. 5). (*Open symbols*) In relaxing solution. (*Filled symbols*) In rigor solution. Lines are pressure/spacing curves calculated from the electrostatic model assuming thick filament compression and an attractive force as described in the text, for sarcomere lengths of 3.6 and 2.2 μm. (*Dashed lines*) Relaxing conditions. (*Solid lines*) Rigor conditions.

CONCLUSIONS

In the filament lattice of vertebrate cross-striated muscle the predominant repulsive force appears to be electrostatic, although we cannot fully exclude other force systems. The repulsive forces may be calculated to a first approximation by assuming that the charge sits on smooth, uniformly-charged cylinders (Millman and Nickel, 1980). In both relaxed and rigor conditions, the thick filament projections are pushed up against the backbone by compressive forces; a greater compressive force is required in rigor than in relaxation.

If the primary repulsive forces on the lattice are electrostatic, one can ask where these charges are situated. In the case of the thin filaments, it seemed reasonable to assign the charges to the outer surface, i.e., at a diameter of 9 nm (see Egelman, 1985). For the thick filaments, comparing the effective charge diameter (26 nm) with the expected backbone diameter (~15 nm) and the radial position of thick filament projections as determined by x-ray diffraction and electron microscopy (Haselgrove, 1980; Kensler and Stewart, 1983; Stewart and Kensler, 1986), the charge producing the repulsion would appear to be situated on HMM, probably near the center of the S-1 part. Determination of electron density distributions across the lattice show that there is a shift of mass (probably HMM-S1) from the region of the thick filaments to that of the thin filaments when a muscle moves from relaxation to rigor or contraction (Huxley, 1968; Haselgrove and Huxley, 1973). If, during this move, charge and charge distribution (on HMM) were to remain unchanged, a significant increase in radial repulsive pressure would be observed. As well,

when the muscle moves from relaxation to rigor, the net charge on the thick filaments appears to increase, with only little change in the thin filament charge (Bartels et al., 1984), an observation which would imply a further increase the repulsive force. Since no increase in force is observed, we conclude that the charge (and particularly the outermost charge) on the thick filaments is not at the same position in rigor as in relaxed muscle, relative to the filament backbone. Since when the muscle shifts from relaxation to rigor, the projections move towards the thin filaments, this means that the effective charge must shift on the projections away from the ends of the HMM-S1.

We plan to extend this study to the contracting state and to investigate the effects of lattice spacing and external pressure on the contraction process. It has been shown that lattice compression can interfere with muscle contraction, but at the moment the details of this interference are not clear (Maughan and Godt, 1981; Gulati and Babu, 1985; Diamond et al., 1986).

We are grateful to Drs. E. M. Bartels, G. F. Elliott, J. C. Haselgrove, B. G. Nickel, and K. Wakabayashi for helpful discussions and to Rosalind Blair for technical assistance.

This work was done with grant support from the Natural Science and Engineering Research Council of Canada.

Received for publication 31 July 1987 and in final form 18 April 1988.

REFERENCES

April, E. W. 1975. Liquid-crystalline characteristics of the thick filament lattice of striated muscle. *Nature (Lond.)*. 257:139–141.

April, E. W., and D. W. Maughan. 1986. Active force as a function of filament spacing in crayfish skinned muscle fibers. *Pfluegers Arch. Eur. J. Physiol.* 407:456–460.

April, E. W., and J. Schreder. 1979. Role of osmotic forces in myofilament lattice stability in striated muscle. *Biophys. J.* 25:18*a*. (Abstr.)

April, E. W., and D. Wong. 1976. Non-isovolumic behavior of the unit cell of skinned striated muscle fibers. *J. Mol. Biol.* 101:107–114.

Bartels, E. M., P. H. Cooke, G. F. Elliott, and R. A. Hughes. 1984. Donnan potential changes in rabbit muscle A-bands are associated with myosin. *J. Physiol. (Lond.)*. 358:80*a*. (Abstr.)

Bartels, E. M., and G. F. Elliott. 1985. Donnan potentials from the A- and I-bands of glycerinated and chemically-skinned muscles, relaxed and in rigor. *Biophys. J.* 48:61–76.

Brenner, B., L. C. Yu, and R. J. Podolsky. 1984. X-ray diffraction evidence for cross-bridge formation in relaxed muscle fibers at various ionic strengths. *Biophys. J.* 46:299–306.

Brenner, S. L., and D. A. McQuarrie. 1973. Force balances in systems of cylindrical polyelectrolytes. *Biophys. J.* 13:301–331.

Cooke, P. H., E. M. Bartels, G. F. Elliott, and R. A. Hughes. 1987. A structural study of gels, in the form of threads, of myosin and myosin rod. *Biophys. J.* 51:947–957.

Diamond, M. S., P. W. Brandt, and M. Kawai. 1986. Comments on Critical dependence of calcium-activated force on width in highly compressed skinned fibers of the frog. *Biophys. J.* 50:1215–1216.

Duncan, C. J. 1987. Role of calcium in triggering rapid ultrastructural damage in muscle: a study with chemically skinned fibres. *J. Cell Sci.* 87:581–594.

Egelman, E. H. 1985. The structure of actin. *J. Musc. Res. Cell Motil.* 6:129–151.

Elliott, G. F. 1980. Measurement of the electric charge and ion-binding of the protein filaments in intact muscle and cornea, with implications for filament assembly. *Biophys. J.* 32:95–97.

Elliott, G. F., J. Lowy, and C. R. Worthington. 1963. An X-ray and light-diffraction study of the filament lattice of striated muscle in the living state and in rigor. *J. Mol. Biol.* 6:295–305.

Elliott, G. F., J. Lowy, and B. M. Millman. 1967. Low-angle X-ray diffraction studies of living striated muscle during contraction. *J. Mol. Biol.* 25:31–45.

Elliott, G. F., and E. M. Rome. 1969. Liquid-crystalline aspects of muscle fibers. *Mol. Cryst. Liq. Cryst.* 8:215–218.

Godt, R. E., and D. W. Maughan. 1977. Swelling of skinned muscle fibers of the frog. *Biophys. J.* 19:103–116.

Gulati, J., and A. Babu. 1985. Critical dependence of calcium-activated force on width in highly compressed skinned fibers of the frog. *Biophys. J.* 48:781–787.

Haselgrove, J. C. 1980. A model of myosin crossbridge structure consistent with the low-angle X-ray diffraction pattern of vertebrate muscle. *J. Musc. Res. Cell Motil.* 1:177–191.

Haselgrove, J. C., and H. E. Huxley. 1973. X-ray evidence for radial crossbridge movement and for the sliding filament model in actively contracting skeletal muscle. *J. Mol. Biol.* 77:549–568.

Higuchi, H., and Y. Umazume. 1986. Lattice shrinkage with increasing resting tension in stretched, single-skinned fibers of frog muscle. *Biophys. J.* 50:385–389.

Huxley, A. F., and L. D. Peachey. 1961. The maximum length for contraction in vertebrate striated muscle. *J. Physiol. (Lond.)*. 156:150–165.

Huxley, H. E. 1968. Structural difference between resting and rigor muscle; evidence from intensity changes in the low-angle equatorial X-ray diagram. *J. Mol. Biol.* 37:507–520.

Huxley, H. E., and W. Brown. 1967. The low-angle X-ray diagram of vertebrate striated muscle and its behavior during contraction and rigor. *J. Mol. Biol.* 30:383–434.

Irving, T. C. 1983. Radial forces in the filament lattice of vertebrate striated muscle. M.Sc. thesis. University of Guelph, Canada.

Irving, T. C., and B. M. Millman. 1983. Interfilament forces in vertebrate striated muscle at long sarcomere lengths. *Biophys. J.* 41:253*a*. (Abstr.)

Irving, T. C., and B. M. Millman. 1984. Effects of low ionic strength on interfilament forces in striated muscle. *Biophys. J.* 45:101*a*. (Abstr.)

Irving, T. C., and B. M. Millman. 1985. Structural changes in the thick filaments of frog skeletal muscle as external pressure of the filament lattice is varied. *Biophys. J.* 47:127*a*. (Abstr.)

Irving, T. C., and B. M. Millman. 1987. The filament lattice of vertebrate striated muscle. Modeling filament position and cross-bridge movement. *Biophys. J.* 51:471*a*. (Abstr.)

Kensler, R. W., and M. Stewart. 1983. Frog skeletal muscle thick filaments are three-stranded. *J. Cell Biol.* 96:1797–1802.

Magid, A., and M. K. Reedy. 1980. X-ray diffraction observations of chemically-skinned frog skeletal muscle processed by an improved method. *Biophys. J.* 30:27–40.

Matsubara, I., and G. F. Elliott. 1972. X-ray diffraction studies on skinned single fibres of frog skeletal muscle. *J. Mol. Biol.* 72:657–669.

Matsubara, I., Y. E. Goldman, and R. M. Simmons. 1984. Changes in the lateral filament spacing of skinned muscle fibres when cross-bridges attach. *J. Mol. Biol.* 173:15–33.

Matsuda, T., and R. J. Podolsky. 1984. X-ray evidence for two structural states of the actomyosin cross-bridge in muscle fibers. *Proc. Natl. Acad. Sci. USA.* 81:2364–2368.

Maughan, D. W., and R. E. Godt. 1981. Radial forces within muscle fibers in rigor. *J. Gen. Physiol.* 77:49–64.

Millman, B. M. 1981. Filament lattice forces in vertebrate striated muscle: relaxed and in rigor. *J. Physiol. (Lond.)*. 320:118*a*. (Abstr.)

Millman, B. M. 1986. Long-range electrostatic forces in cylindrical systems: muscle and virus gels. *In* Electrical Double Layers in Biology. M. Blank, editor. Plenum Publishing Corp., New York. 301–312.

Millman, B. M., and R. M. Bell. 1983. Lateral forces between actin filaments in muscle. *Biophys. J.* 41:253*a*. (Abstr.)

Millman, B. M., and T. C. Irving. 1980. Interfilament forces in the lattice of vertebrate striated muscle. *Fed. Proc.* 39:1731*a*. (Abstr.)

Millman, B. M., and T. C. Irving. 1982. Lateral cross-bridge forces in striated muscle. *Biophys. J.* 37:364*a*. (Abstr.)

Millman, B. M., and T. C. Irving. 1986. Modeling radial forces in the muscle filament lattice. *Biophys. J.* 49:80*a*. (Abstr.)

Millman, B. M., T. C. Irving, B. G. Nickel, and M. Loosley-Millman. 1984. Interrod forces in aqueous gels of tobacco mosaic virus. *Biophys. J.* 45:551–556.

Millman, B. M., T. J. Racey, and I. Matsubara. 1981. Effects of hyperosmotic solutions on the filament lattice of intact frog skeletal muscle. *Biophys. J.* 33:189–202.

Millman, B. M., and B. G. Nickel. 1980. Electrostatic forces in muscle and cylindrical gel systems. *Biophys. J.* 32:49–63.

Millman, B. M., and T. J. Racey. 1977. Osmotic shrinkage of the filament lattice in frog semitendinosus muscle. *Biophys. J.* 17:175*a*. (Abstr.)

Millman, B. M., and K. Wakabayashi. 1979. Shrinking of the muscle filament lattice in polymeric solutions. *Biophys. J.* 25:111*a*. (Abstr.)

Millman, B. M., K. Wakabayashi, and T. J. Racey. 1983. Lateral forces in the filament lattice of vertebrate striated muscle in the rigor state. *Biophys. J.* 41:259–267.

Naylor, G. R. S., E. M. Bartels, T. D. Bridgman, and G. F. Elliott. 1985. Donnan potentials in rabbit psoas muscle in rigor. *Biophys. J.* 48:47–59.

Padron, R., and H. E. Huxley. 1984. The effect of the ATP analogue AMPPNP on the structure of crossbridges in vertebrate skeletal muscles: x-ray diffraction and mechanical studies. *J. Musc. Res. Cell Motil.* 5:613–655.

Pepe, F. A. 1967. The myosin filament. II. Interaction between myosin and actin filaments observed using antibody staining in fluorescent and electron microscopy. *J. Mol. Biol.* 27:227–236.

Perrin, D. D., and I. G. Sayce. 1967. Computer calculations of equilibrium concentrations in mixtures of metal ions and complexing species. *Talanta* 14:833–842.

Schoenberg, M. 1980. Geometrical factors influencing muscle force development. II. Radial forces. *Biophys. J.* 30:69–78.

Stewart, M., and R. W. Kensler. 1986. Arrangement of myosin heads ion relaxed thick filaments from frog skeletal muscle. *J. Mol. Biol.* 192:831–851.